Electronic Supplementary Material (ESI) for RSC Advances

Solvatochromic fluorescent cyanophenoxazine: design, synthesis, photophysical properties and fluorescence light-up sensing of ct-DNA

Subhendu Sekhar Bag,* Samir Ghorai, Subhashis Jana and Chandan Mukherjee*

Department of Chemistry, Indian Institute of Technology, Guwahati-781039, India.
Ph.: (+) 91-361-258-2324/2327, Fax: (+) 91-361-258-2349.
E-mail: ssbag75@iitg.ernet.in// cmukherjee@iitg.ernet.in

1. Experimental Section

1.1. General Methods

All reactions were carried out under a nitrogen atmosphere in flame-dried glassware using nitrogen filled balloon. Organic extracts were dried over anhydrous sodium sulphate. Solvents were removed in a rotary evaporator under reduced pressure. Silica gel (60-120 mesh size) was used for the column chromatography. Reactions were monitored by TLC on silica gel 60 F254 (0.25mm). ^{1}H NMR spectra were recorded at 400 MHz spectrometer and ^{13}C NMR spectra were recorded at 100 MHz spectrometer. Coupling constant (*J* value) was reported in hertz. The chemical shifts were shown in ppm downfield from tetramethylsilane, using residual chloroform ($\delta = 7.24$ in ^{1}H NMR, $\delta = 77.23$ in ^{13}C NMR), dimethyl sulfoxide ($\delta = 2.5$ in ^{1}H NMR, $\delta = 39.5$ in ^{13}C NMR), as an internal standard. Mass spectra were recorded using HR mass spectrometer and data analyzed using the inbuilt software. IR spectra were recorded in KBr or neat on a FT-IR spectrometer.

1.2. Crystallographic Description

Crystal data were collected with a CCD diffractometer using graphite monochromatedMoKα radiation ($\lambda = 0.71073$ Å) at 298 K. Cell parameters were retrieved using and refined with softwares on all observed reflections. Data reduction was performed with the software and corrected for Lorentz and polarization effects. Absorption corrections were applied with the program. The structure was solved by direct methods implemented in a program and refined by full-matrix least-squares methods on F2. All non-hydrogen atomic positions were located in difference Fourier maps and refined anisotropically. The hydrogen atoms were placed in their geometrically generated positions. colourless crystals were isolated in rectangular shape from acetonitrile at room temperature.

1.3. Synthetic Procedure and Characterization Data

1.3.1. Synthetic Scheme

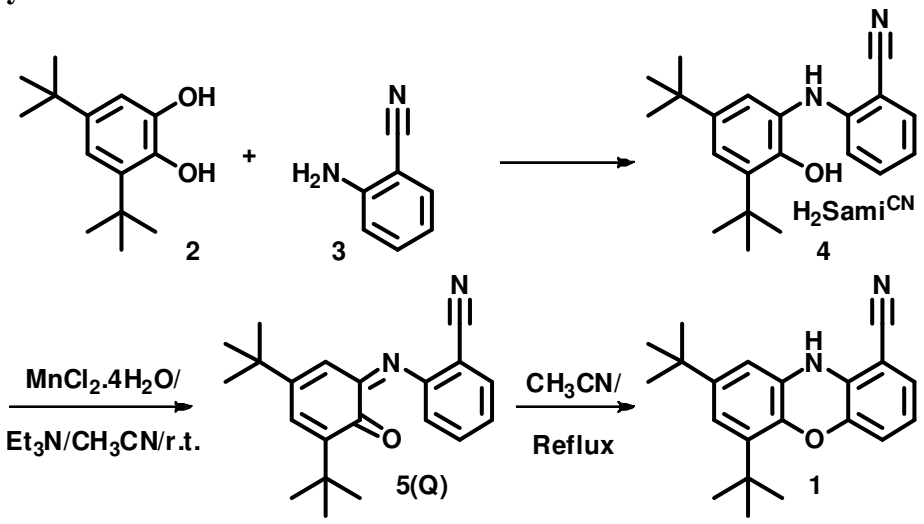

Scheme S1: Synthesis of donor and/or acceptor substituted classical Phenoxazine fluorophore.

1.3.2. Synthesis of (Z)-2-(3,5-di-tert-butyl-6-oxocyclohexa-2,4-dienylideneamino)benzonitrile (5): A 25:1 (*i.e.* 4 mol%) mixture of H_2Sami^{CN} (**4**, 0.161 g, 0.50 mmol)[1] and $MnCl_2 \bullet 4H_2O$ (0.004 g, 0.02 mmol) in CH_3CN (10 mL) was stirred after adding Et_3N (0.10 mL) for 14 h at room temperature (30 °C). The resulting reddish brown solution was filtered through Buchner funnel and slow evaporation of the filtrate provided crystalline compound **5** (**Q**). Yield 0.157 g, 98%; FTIR (KBr pellet, cm^{-1}) 3066, 2967, 2954, 2901, 2862, 2221, 1665, 1627, 1586, 1557, 1474, 1376, 1274, 897, 768, 760; ^1H NMR ($CDCl_3$, 400 MHz) δ 1.13 (s, 9H), 1.33 (s, 9H), 6.00 (d, J = 1.6 Hz, 1H), 6.92 (d, J = 8.0 Hz, 1H), 7.01 (s, 1H), 7.23 (t, J = 7.6 Hz, 1H), 7.57 (t, J = 8.2 Hz, 1H), 7.67 (d, J = 7.2 Hz, 1H); HRMS ES^+ *m/z* calcd for $C_{21}H_{25}N_2O_1$ $[M+H]^+$ 320.1967, found 320.1710.

The resulting oxidized compound **Q** (**5**, 0.155 g, 0.48 mmol) was further heated to reflux in CH_3CN (15 mL) for 19 h. After cooling to room temperature, resulting solution, having fluorescence property, was filtered and kept for slow evaporation. A faint−yellow crystalline compound **1**was obtained in 96% yield (0.149 g).

1.3.3. Synthesis of 6,8-di-tert-butyl-10H-phenoxazine-1-carbonitrile (1): To a stirred solution of H_2Sami^{CN} (**4**, 0.161 g, 0.5 mmol) in CH_3CN (15 mL) was added $MnCl_2 \bullet 4H_2O$

(0.106 g, 0.53 mmol). Addition of Et_3N (0.10 mL), solution colour immediately turned to reddish brown. The homogeneous solution was then heated to reflux for 8 h. After filtration at room temperature the filtrate was kept for slow evaporation which provided yellow crystalline solid of desired product **1** suitable for single crystal X–ray crystallography. Yield 0.110 g, 69%; FTIR (KBr pellet) 3318, 2961, 2902, 2866, 2226, 1626, 1576, 1484, 1438, 1361, 1319, 1287, 1246, 860, 774, 723 cm^{-1}; ^1H NMR ($CDCl_3$, 400 MHz) δ 1.20–1.25 (m, 9H), 1.32–1.37 (m, 9H), 5.82 (s, 1H), 6.42 (d, J = 1.6 Hz, 1H), 6.56–6.64 (t, J = 1.6 Hz, 1H), 6.78–6.83 (t, J = 1.0 Hz, 2H), 6.85–6.92 (m, 1H) ppm. ^{13}C NMR ($CDCl_3$, 100 MHz) δ 30.0, 31.5, 34.6, 34.9, 94.8, 110.3, 116.5, 117.8, 119.1, 120.7, 125.8, 129.4, 136.8, 137.1, 139.4, 144.16, 146.5 ppm; HRMS ES^+ *m/z*: calcd. for $C_{21}H_{24}N_2O_1$ [M^+] 320.1889, found 320.1640.

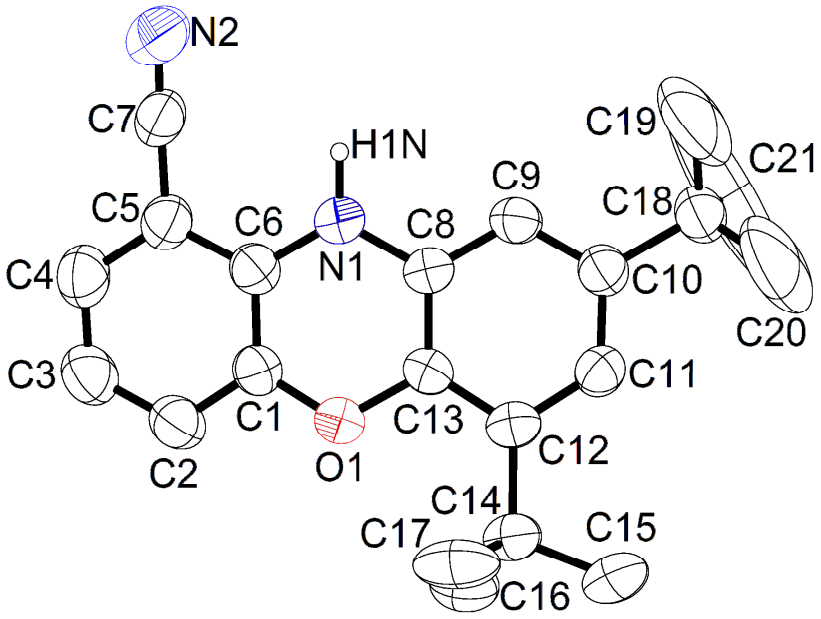

Figure S1. An ORTEP representation of **1**; ellipsoids were drawn at 50% probability level. The *tert*-butyl group comprised of C18, C19, C20, and C21 showed some sort of disorderness. Hydrogens except H1N were not shown.

Table S1. Crystallographic data and structure refinement for **1**.

Empirical formula	$C_{21}H_{24}N_2O$
Formula weight	320.42
Crystal habit, colour	block / yellow
Crystal size, mm	0.44 X 0.36 X 0.18
Temperature, T	296(2) K
Wavelength, λ	0.71073 Å
Crystal system	Monoclinic
Space group	*C 1 2/c 1*
Unit cell dimensions	a = 34.3374(12) Å b = 6.0181(2) Å c = 18.6307(6) Å $\alpha = \gamma = 90°$, $\beta = 104.012(2)°$
Volume, V	3735.4(2) $Å^3$
Z	8
Calculated density	1.140 $Mg \cdot m^{-3}$
Absorption coefficient, μ	0.070 mm^{-1}
$F(000)$	1376
θ range for data collection	1.22 to 25.00°
Limiting indices	$-33 \le h \le 37$, $-7 \le k \le 7$, $-20 \le l \le 22$
Reflection collected / unique	20752 / 3093 [R(int) = 0.0314]
Completeness to θ	94 % (θ = 25.00°)
Refinement method	'SHELXL-97 (Sheldrick, 1997)'
Data / restraints / parameters	3093 / 0 / 229
Goodness-of-fit on F^2	1.053
Final R indices [I>2sigma(I)]	$R1$ = 0.0856, $wR2$ = 0.2631
R indices (all data)	$R1$ = 0.1038, $wR2$ = 0.2862
Largest diff. peak and hole	0.594 and –0.511 $e \cdot Å^{-3}$

Table S2. Selected bond distances (Å) and bond angles (°) for **1**.

C1–C2	1.365(5)	C10–C11	1.391(4)
C2–C3	1.391(5)	C11–C12	1.397(5)
C3–C4	1.368(5)	C12–C13	1.385(4)
C4–C5	1.401(5)	C13–C8	1.390(4)
C5–C6	1.390(5)	N1–C6	1.378(5)
C6–C1	1.401(4)	N1– C8	1.401(4)
C5–C7	1.435(5)	N2– C7	1.141(5)
C8–C9	1.381(5)	O 1–C1	1.374(4)
C9–C10	1.376(4)	O1– C13	1.392(4)

N1–C8–C13	119.03(28)	C1–C6–N1	118.28(28)
C8–C13–O1	119.24(26)	C6–N1–C8	119.68(28)
O1–C1–C6	120.26(28)		

X–ray single–crystal structural examination at 296(2) K showed that **1** crystallized in the space group *C*12/*c*1. The two C_6 rings are fused by an amine nitrogen and an oxide oxygen units at 5 (N1) and 10 (O1) positions (Fig 1A). The angle between the two C_6 ring planes is ~ 13 °. The C–C bond distances of the C_6 rings unambiguously indicated their phenyl form Furthermore, C–N and C–O bond distances [C6–N1, 1.376(5); C8–N1, 1.401(5); C1–O1, 1.375(4); C13–O1, 1.394(5)] are in accord with their single bond character (ESI†). Therefore, the compound was a well description of a phenoxazine derivative where one phenyl ring contained two *tert*–butyl groups at –*ortho* and –*para* positions and the second phenyl ring contained a cyanide group at –*meta* position compared to the bridging oxygen atom.

2. Study of Photophysical Properties

2.1. UV-visible and Fluorescence Measurements

All UV-visible spectra of the compound (10 μM) was measured in different solvents of varying dielectric constant by UV-visible spectrophotometer using 1 cm path length cell at 298 K. Fluorescence spectra of the compounds (10 μM) were measured in different solvents of varying dielectric constant by fluorescence spectrophotometer at 298 K using 1 cm path length cell. Time resolved fluorescence decays were measured using time resolved fluorescence spectrophotometer. The fluorescence quantum yields (Φ_f) were determined using quinine sulphate as a reference with the known Φ_f= 0.54 in 0.1 molar solution in sulphuric acid.

2.2. UV-visible and fluorescence spectra

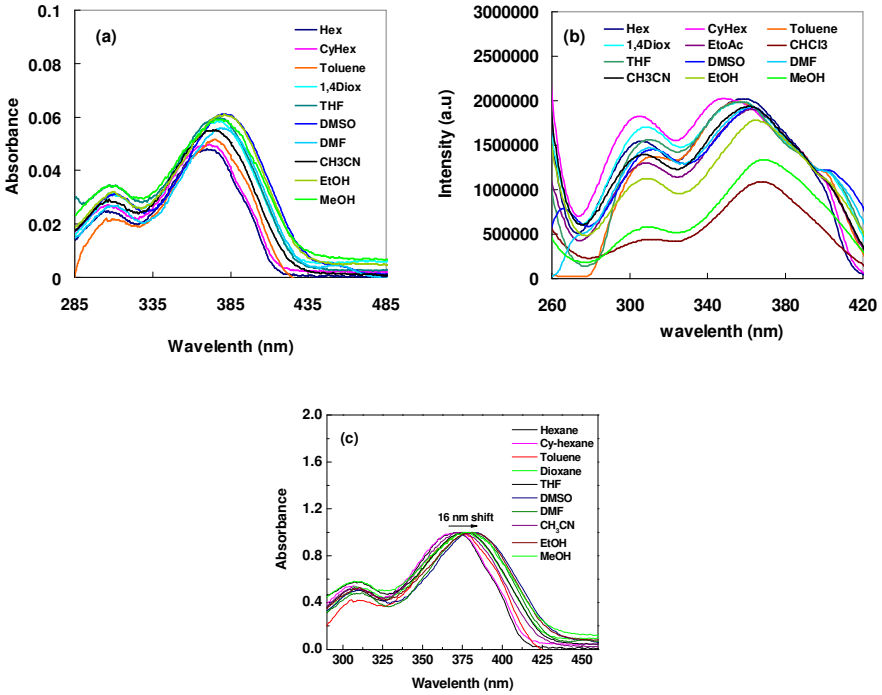

Figure S2. UV-Visible (a), Excitation spectra (b) and (c) Normalized UV-Visible spectra of Phenoxazine in different solvents (10 µM, r.t.; λ_{ex} = 370nm – 380 nm).

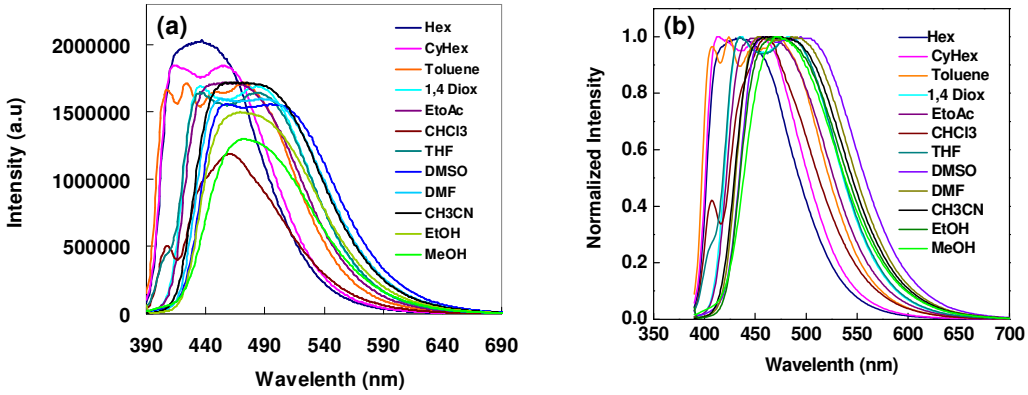

Figure S3a. Fluorescence spectra (a) and Normalized fluorescence spectra (b) of Phenoxazine in different solvents (10 µM, r.t.; λ_{ex} = 370nm – 380 nm).

2.3. Concentration dependent absorption and emission in buffer

To characterize that the fluorophore does not form any aggregation or the feasibility of quantifying the titration experiment for calculating association constant, we subsequently studied the spectral parameters over a broad range of concentrations. Figure S3b fluorescence spectra of the probe over the concentration range of 6-36 μM in phosphate buffer of pH 7.0 in presence of ct-DNA. The fluorescence spectra did not change in band position. Moreover, the fluorescence intensities depend linearly on the concentration of the probe in solution, suggesting that the triazolylpyrene exists in a monomeric state and no aggregation is formed. These linear relationships allowed us to fit fluorescence titration curve data quantitatively to derive the association constants of probe-/DNA complex with no harm.

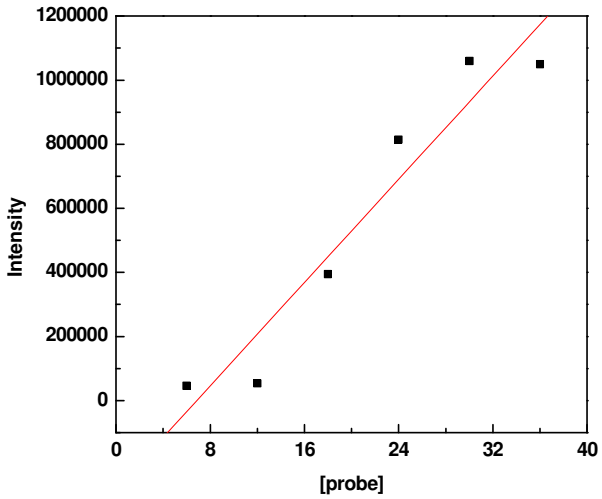

Figure S2b: (a) Plot of fluorescence intensity vs. concentration of the probe in 50mM phosphate buffer of pH 7.0 showing linear relationship in the concentration range shown.

2.4. Photophysical Summary of the Fluorophore

Table S3: Summary table of photophysical properties of the fluorophore.

Entry	Solvents	Δf	UV-Vis & Fluorescence		
			λ_{max}^{abs} (nm)	λ_{max}^{fl} (nm)	Φ_f
1	Cyclohex	0.000	309, 373	415, 457	0.72
	Hexane	0.001	308, 373	437	0.78
	Toluene	0.013	312, 377	426, 449, 475	0.79
	Dioxane	0.021	312, 377	437, 485	0.68
	$CHCl_3$	0.148	310, 393	460	0.31
	EtOAc	0.201	311, 377	460	0.27
	THF	0.210	310, 385	437, 486	0.36
	DMSO	0.265	312, 384	460, 503	0.37
	DMF	0.275	311, 382	455, 495	0.30
	EtOH	0.290	311, 383	474	0.18
	ACN	0.307	310, 375	473	0.39
	MeOH	0.309	310, 379	477	0.15

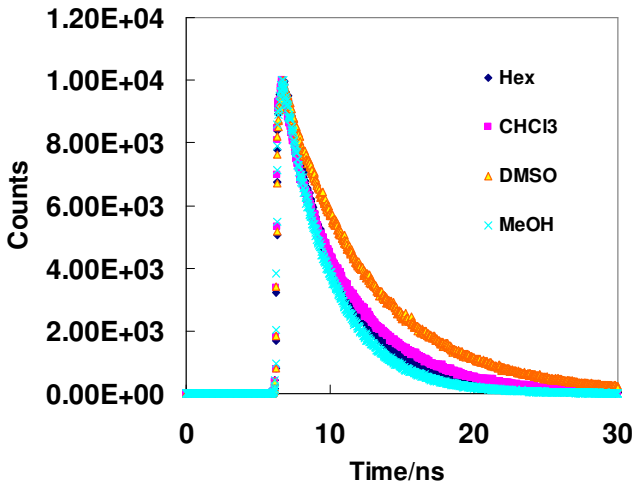

Figure S4a: Time resolved fluorescence spectra of fluorophore in different solvent of varying polarity.

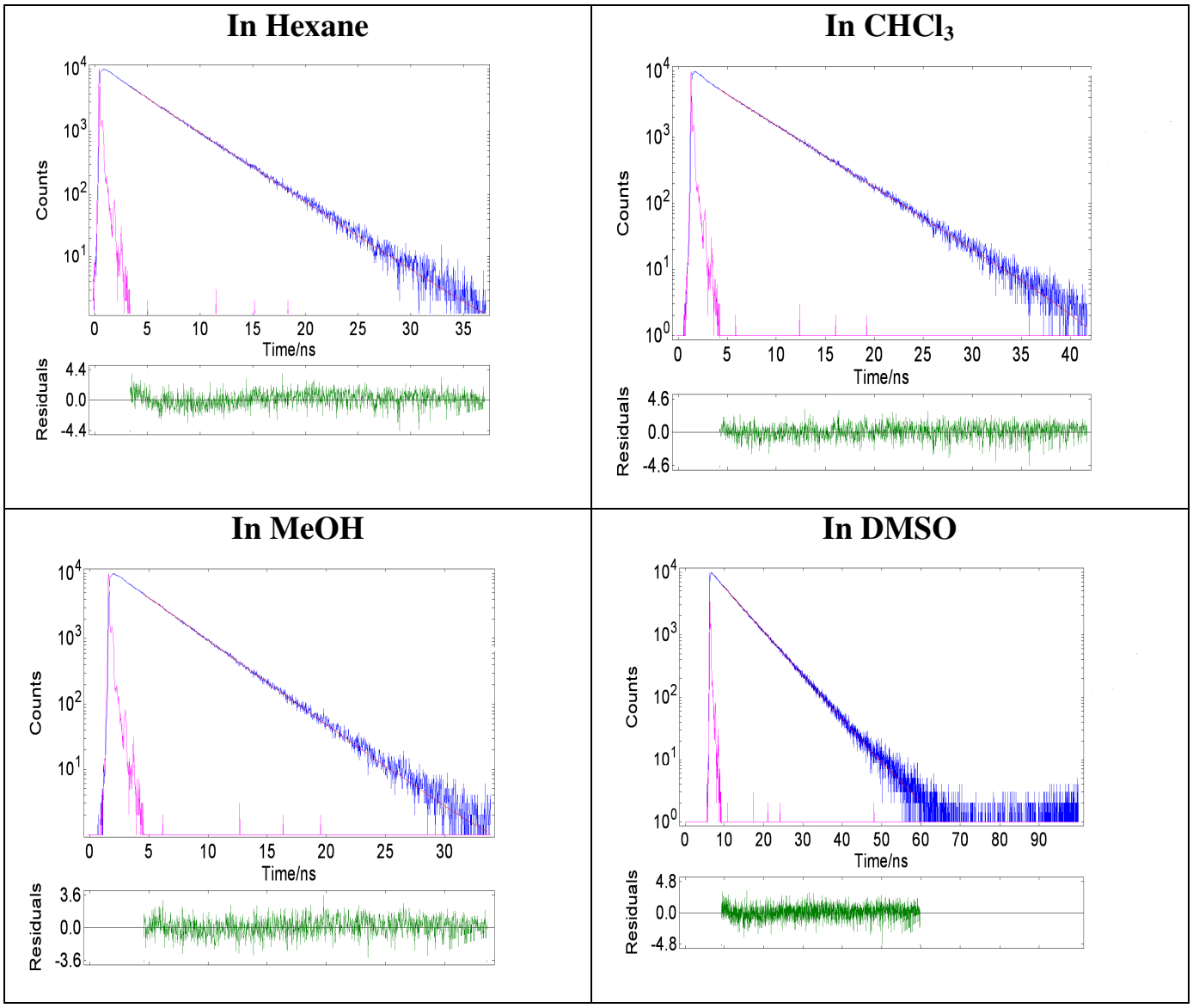

Figure S4b: **Time resolved fluorescence spectra: Goodness of fit Graphs in different solvents.**

Table S4: Summary table of fluorescence lifetimes of the fluorophores

Entry	Solvents	Φ_f	λ [nm]	τ_1 [ns]	τ_2 [ns]	$<\tau>$ [ns]	k_f [$10^8 s^{-1}$]	k_{nr} [$10^8 s^{-1}$]	χ^2
1	Hexane	0.78	440	3.9 (100%)	----	3.9	1.9	0.5	1.2
	Chloroform	0.31	460	4.6 (100%)	----	4.6	0.7	1.5	1.0
	MeOH	0.15	480	3.4 (100%)	----	3.4	0.4	2.5	1.1
	DMSO	0.37	500	6.1 (100%)	----	6.1	0.6	1.0	1.2
	Phosphate buffer(pH-7.0)	0.002	440	8.7 (87.5%)	4.8 (12.5%)	8.0	0.002	1.2	1.1

2.5. Lippert and Mataga Plots

The Lippert-Mataga polarity parameter (Δf) has been considered as the measure of the polarity of different solvents and solvent mixtures used and was calculated using following equation.

$$\Delta f = \frac{\varepsilon - 1}{2\varepsilon + 1} - \frac{n^2 - 1}{2n^2 + 1} \qquad (1)$$

In different solvents, the absorption and fluorescence spectra involve the electronic transitions between the same two ground and excited electronic states, the Stokes' shift ($\Delta\tilde{\nu}$) is expected to follow a linear relation with Δf, as suggested by the Lippert and Mataga equation as

$$\Delta\tilde{\nu} = \Delta\tilde{\nu}_0 + \frac{2(\mu_e - \mu_g)^2}{hca^3}\Delta f \qquad (2)$$

where μ_e and μ_g are the excited (fluorescent) state and the ground state dipole moments of the fluorophore, h is Planck's constant, c is the velocity of light, and a is the Onsager radius of the dipole-solvent interaction sphere. The $\Delta\tilde{\nu}$ values for the compound in different solvents were estimated (in cm^-

[1]) considering the λ_{max}^{abs} and λ_{max}^{fl} values from non-polar to polar or low polar to high polar solvents. The $\Delta\tilde{\nu}$ values thus estimated for the phenoxazine fluorophore.

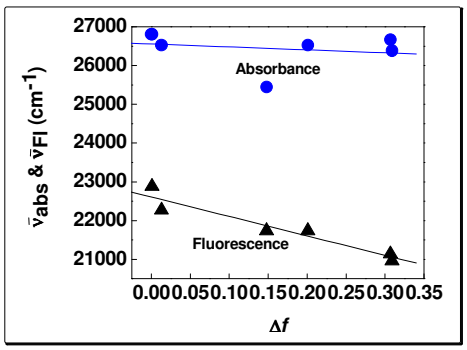

Figure S5: Plot of $\tilde{\nu}_{abs}$& $\tilde{\nu}_{Fl}$ values against solvent polarity parameter Δf for the fluorophore **.**

Table S5: Summary table of $\tilde{\nu}_{max}^{abs}$ and $\tilde{\nu}_{max}^{fl}$ of the fluorophore and fluorescent nucleoside and solvent polarity parameter (Δf).

Solvent	Δf	$\tilde{\nu}_{max}^{abs}$ (cm^{-1})	$\tilde{\nu}_{max}^{fl}$ (cm^{-1})
Cyclohex	0.000	26809.65	24096.39
Hexane	0.001	26809.65	22883.3
Toluene	0.013	26525.2	22271.71
$CHCl_3$	0.148	25445.29	21739.13
EtOAc	0.201	26525.2	21739.13
ACN	0.307	26666.67	21141.65
MeOH	0.309	26385.22	20964.36

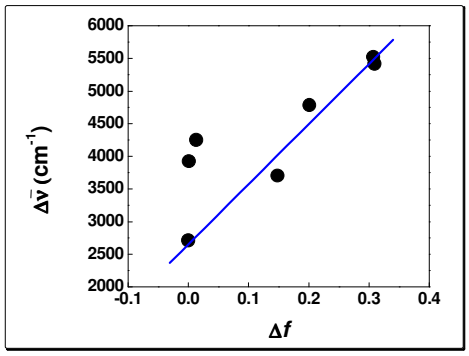

Figure S6: Plots of $\Delta\tilde{\nu}$ values against Δf in different solvents for the fluorophore.

Table S6: Summary table of $\Delta\tilde{v}$ of the fluorophore and solvent polarity parameter (Δf).

Solvent	Δf	$\Delta\tilde{v}$ (cm^{-1})
Cyclohex	0.000	2713.26593
Hexane	0.001	3926.35628
Toluene	0.013	4253.48402
$CHCl_3$	0.148	3706.16219
EtOAc	0.201	4786.0685
ACN	0.307	5525.01762
MeOH	0.309	5420.86369

3. Studies on the interaction of 1 (^{TNDMB}Py) with ct-DNA

3.1. General experimental

3.1.1. Materials

Calf thymus DNA was purchased from Sigma (USA) and used without further purification. Na_2HPO_4 and $NaH_2PO_4.H_2O$ (for preparation of phosphate buffer) were purchased from Merck, India. Water was obtained from a Milli-Q purification system. All experiments were performed with freshly prepared solutions. The probe molecule was purified according to the procedure described. We recrystallised the column purified material in chloroform-ethylacetate solvent mixture twice, dried under vacuum, again characterized and used the very pure material for study.

3.1.2. Preparation of ct-DNA Solution

The supplied ct-DNA was dissolved in 1 ml Milli-Q water and reconstituted overnight at 2 – 8 ^{o}C to dissolve all the material and then and filtered through a 0.45 µm filter. The DNA concentration was determined by measuring the absorbance at 260 nm (A_{260}) and using the following formula: [2]

µg/mL of ct-DNA = A_{260} x 50 µg/ml x Dilution factor

A_{260} = absorbance of the DNA solution at 260 mn

50 µg/mL = the concentration of 1 A_{260} unit of double strand DNA

Thus, from the above formula we can determine the concentration of our stock ct-DNA solution as below:

where, A_{260} = 1.197 and dilution factor = 25

µg/mL of ct-DNA = 1.197 x 50 µg/mL x 25 = 1.4 mg/mL

Thus, the concentration of our stock ct-DNA solution was 1.4 mg/mL. The molar concentration of ct-DNA was determined from UV-visible spectra using molar

absorption coefficient (ε) of 6600 lit mol^{-1} cm^{-1} at 260 nm which was found to be 4536.7 µM. The purity of ct-DNA was checked by UV-visible spectroscopy by measuring the ratio of absorbances at 260 nm to 280 nm which was found to be 1.8 – 1.9 indicating that the ct-DNA is sufficiently free of protein.[2] From that stock solution sub stock of 2000 µM ct-DNA was prepared.

The compound stock solution was prepared in DMF because of the poor solubility in water. 0.01 gm of triazolyl pyrene compound was dissolved in 5 mL DMF to make a stock probe solution of concentration 5154.64 µM.

3.1.3. General experimental on interaction study of ct-DNA by photophysical study: All the spectral measurements were carried out at room temperature. To study the interaction of compound with ct-DNA, an aqueous solution of compound (50 µM for ct-DNA) was titrated with different concentrations of ct-DNA (ranging from 0, 15, 30 … to 90 µg/mL). The total volume of the final solution for each sample was 1 mL. The % of DMF content did not exceed 3%. The presence of ≤3% DMF does not induce changes to biomolecules. Each sample solution was mixed well before spectral measurements.

3.1.4. Photophysical Study: UV-Visible Study

The UV–Visible absorbance measurements were performed using Shimadzu UV - 2550 UV–Visible spectrophotometer with a cell of 1 cm path length at 298 K. All the UV-Visible studies were carried out in 5 mM phosphate buffer of pH 7.0 containing 5 mM NaCl solution at 298 K. 2-3 % DMF was used to solubilize the probe. The measurements were taken in absorbance mode and the absorbance values of the sample solutions were measured in the wavelength regime of 200–600 nm. All the experiments were carried out by freshly prepared sample solutions.

3.1.5. Melting Temperature (*Tm*) Measurements

The melting temperature (*Tm*) of the sample solutions (ct-DNA with probe) were measured in 5 mM sodium phosphate buffer (pH 7.0) containing 5 mM sodium chloride and 1 mM Na_2EDTA. Absorbance *vs*. temperature profiles were measured at 260 nm using a Shimadzu UV-2550 spectrophotometer equipped with a peltier temperature controller using 1 cm path length cell. The absorbance of the samples was monitored at 260 nm from 20 to 90 °C with a heating rate of 1 °C/min. From these profiles, first derivatives were calculated to determine *Tm* values.

3.1.6. Photophysical Study: Fluorescence Study

All fluorescence and steady state anisotropy experiments were performed using a Fluoromax 4 spectrophotometer with a cell of 1 cm path length at 298 K. All the fluorescence studies were carried out in 5 mM phosphate buffer of pH 7.0 containing 5 mM NaCl solution at 298 K. 2-3 % DMF was used to solubilize the

probe. The excitation wavelength for probe (^{TNDMB}**Py**) was set at 343 nm, and emission spectra were measured in the wavelength regime of 350–675.

3.2. UV-visible and Thermal Denaturation, and Fluorescence study of ct-DNA with Phenoxazine Fluorophore.

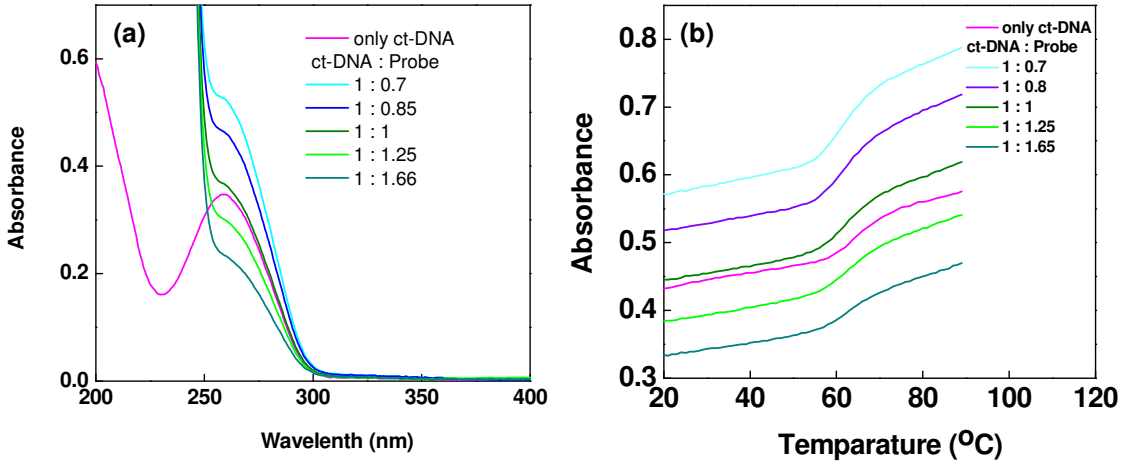

Figure S7: (a) UV-visible spectra of increasing fluorophore concentration in presence of ct-DNA, at room temperature (1eqv = 30 µM), (b) Thermal denaturation study of ct-DNA in presence of fluorophore. [ct-DNA] = 30 µM and [fluorophore] = 21, 25.5, 30, 37.5 and 49.8 µM.

Table S7: Tm values of ct-DNA in presence of Phenoxazine Fluorophore

Entry	ct-DNA : fluorophore	*Tm* (°C)
1	Only ct-DNA	63.2
2	1 : 0.7	60.8
3	1 : 0.85	62.8
4	1 : 1	62.2
5	1 : 1.25	62.4
6	1 : 1.66	61.9

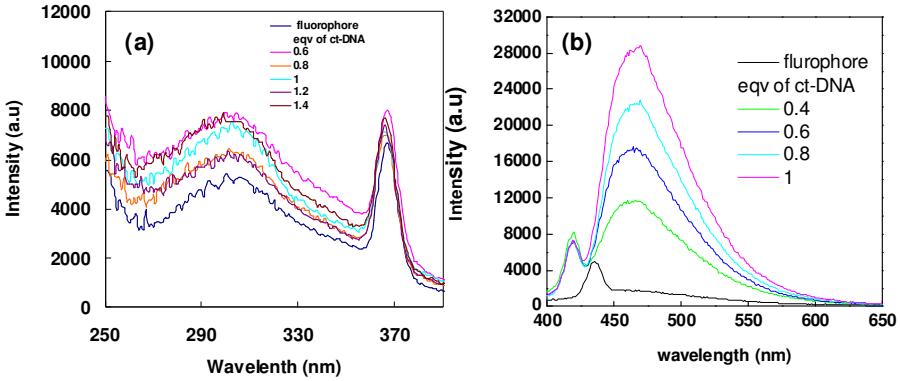

Figure S8: Exitation spectra (a) exited at 420 nm and Emission spectra (b) exited at 366 nm of Fluorophore tritated with increaing concentration of ct-DNA, at room temperature (1eqv = 30 µM).[fluorophore] = 30 µM and [ct-DNA] =18,24, 30, 36 and 42 µM.

Table S8: Summary table of photophysical properties of the fluorophore in presence of ct-DNA.

fluorophore : ct-DNA	UV-Vis & Fluorescence		
	λ_{max}^{abs} (nm)	λ_{max}^{fl} (nm)	Φ_f
1 : 0.4	0.0038	466	0.05
1 : 0.6	0.0037	467	0.07
1:0.8	0.036	468	0.08
1 : 1	0.0031	470	0.13

Table S9: Summary table of fluorescence lifetimes of the fluorophore with Calf Thymas DNA. [λ_{ex} = 366 nm, λ_{em} = 460 nm].

1: ct-DNA	Φ_f	λ [nm]	τ_1[ns]	τ_2[ns]	$<\tau>$ [ns]	k_f [$10^8 s^{-1}$]	k_{nr} [$10^8 s^{-1}$]	χ^2
1 : 0.4	0.05	460	1.04 (77.19%)	4.48 (22.8%)	2.95	0.16	3.22	1.37
1 : 0.6	0.07	460	0.97 (81.98%)	4.62 (18.01%)	2.83	0.24	3.28	1.30
1: 0.8	0.08	465	1.02 (78.96%)	4.62 (21.03%)	2.98	0.30	3.05	1.27
1 : 1	0.13	465	1.1 (77.58%)	4.68 (22.41%)	3.05	0.42	2.85	1.39

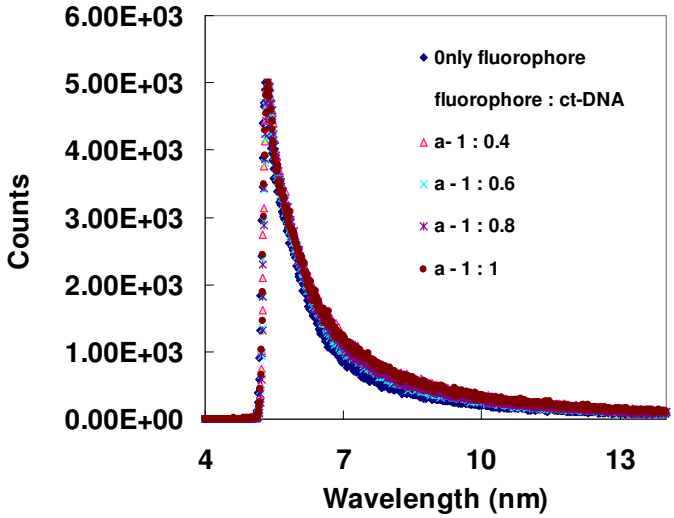

Figure S9a: Time resolved fluorescence spectra of fluorophore with increaing concentration of ct-DNA, at room temperature (1eqv = 30 μM).[fluorophore] = 30 μM and [ct-DNA] =12, 18, 24, 30 μM.

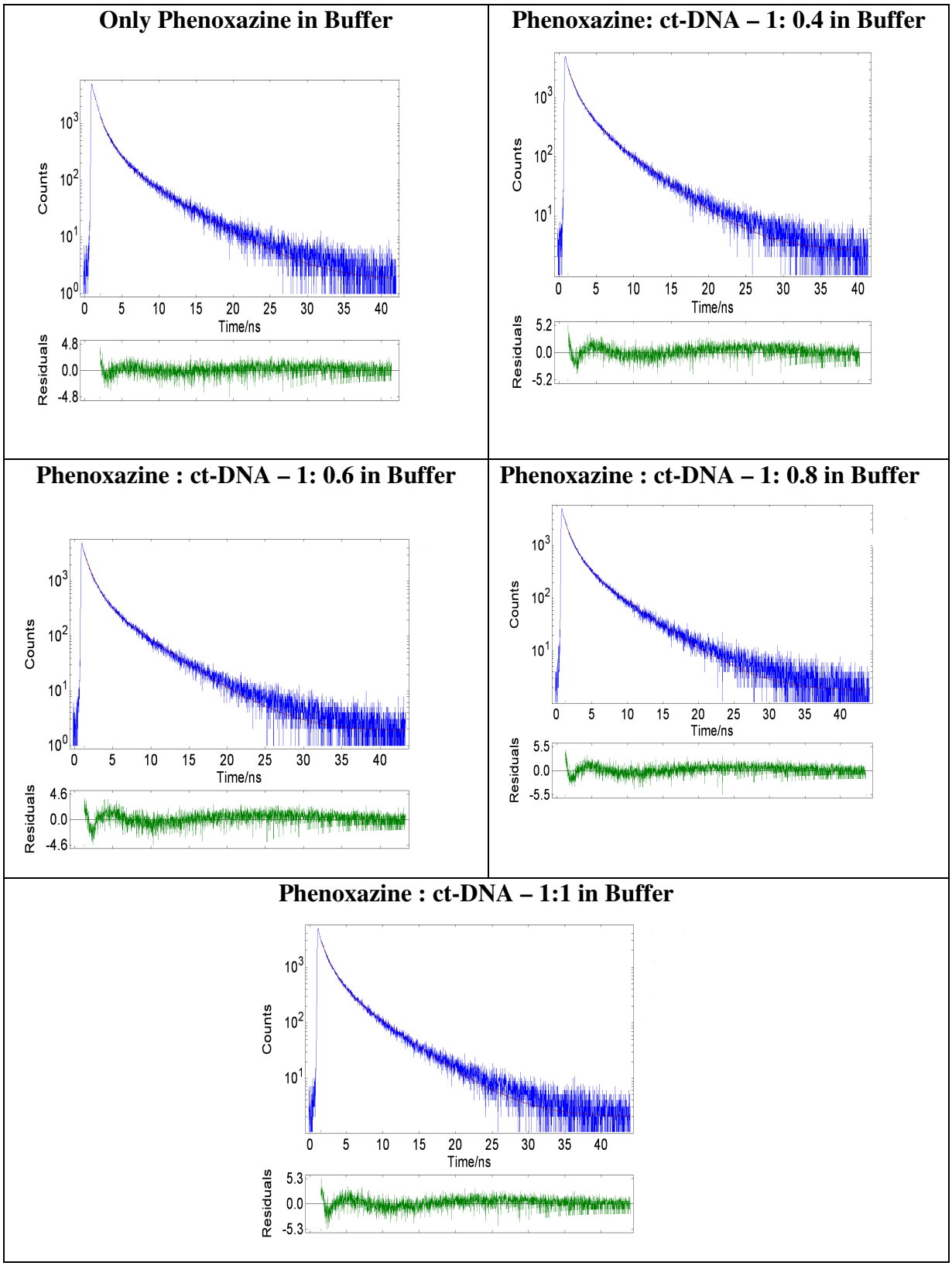

Figure S9b: Time resolved fluorescence spectra: Goodness of fit Graphs in different solvent.

3.3. Benesi-Hildebrand plot to Evaluation Binding Constant

The association constant (K) of the fluorophore with ct-DNA was determind by a Benesi-Hildebrand plot using the following equation 1,

$$\frac{1}{(I-I_o)} = \frac{1}{(I_\alpha - I_o)} + \frac{1}{(I_\alpha - I_o)K[ct-DNA]} \quad \ldots\ldots\ldots\ldots (1)$$

Where I_0, I and I_α are the emission intensities of Phenoxazine fluorophore in the absence of ct-DNA, in the presence of an inetermediate and at infinite concentration of ct-DNA, respectively. From the slop of the $1/(I - I_0)$ *vs.* $1/[\text{ct-DNA}]$ plot of equation 1, binding constant K was determined and its value is 1.34 x 10^4 M^{-1}. The free energy of binding (ΔG) also calculated using the equation 2, it was found to be -5.6 Kcal/mol. $\Delta G = -RT \ln K$ … (2)

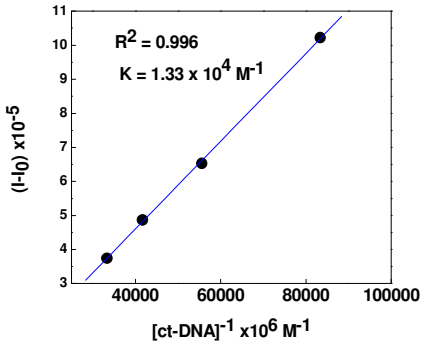

Figure S10a : Benesi- Hildebrand plot of Phenoxazine fluorophore in presence of increasing ct-DNA concentration. . [phenoxazine] = 30 µM and [ct-DNA] = 12, 18, 24 and 30 µM.

3.4. Job's plot from UV-visible study

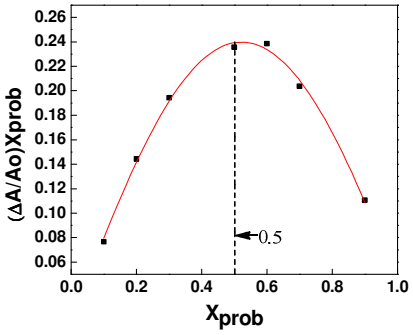

Figure S10b: Job's plot showing 1:1 binding.

3.5. Study of Circular Dichroism (CD) Spectropy

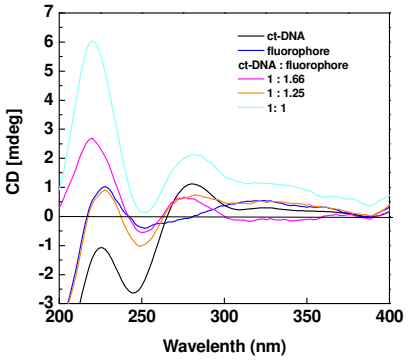

Figure S11: CD spectra of ct-DNA in absence and presence of fluorophore at 298 K. [ct-DNA] =30 µM and [fluorophore] = 18, 24 and 30 µM.

3.6. Evaluation of Binding mode of the probe with ct-DNA by a Dye Displacement Study

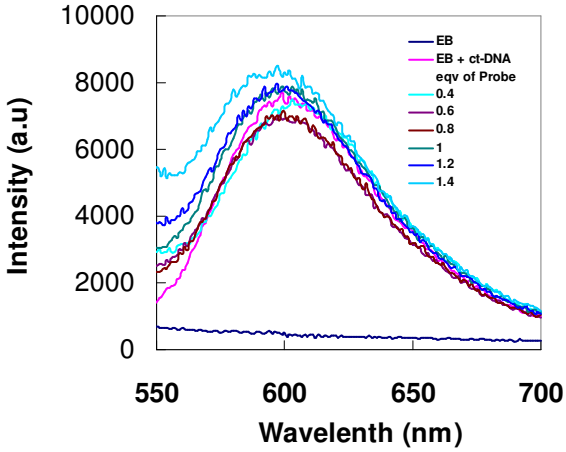

Figure S12: (a) Emission spectra (λ_{ex} = 373 nm) of EB (blue line at bottom), EB-ct-DNA complex and EB-ct-DNA complex mixed with fluorophore**.** [EB] =5 µM, [1 eqv ct-DNA] =25 µM respectively and [Fluorophore**]** =10**,** 15, 20, 25, 30 and 35 µM.

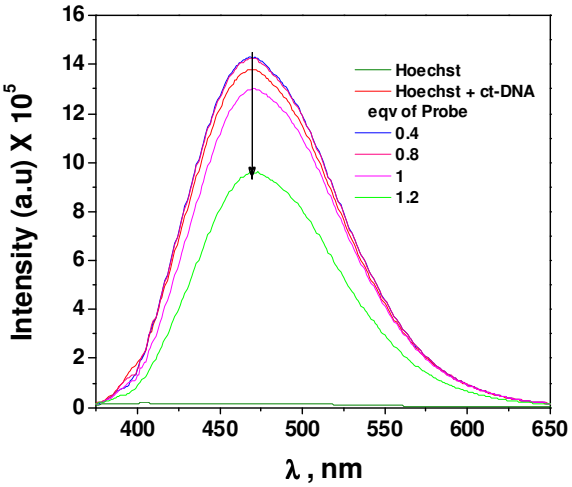

Figure S13: Emission spectra (λ_{ex} = 360 nm) of Hoechst, Hoechst-ct-DNA complex and Hoechst-ct-DNA complex mixed with fluorophore**.** [Hoechst] =5 µM, [1 eqv ct-DNA] =25 µM respectively and [Fluorophore] =10**,** 15, 20, 25, 30 and 35 µM.

3.7. Study of Fluorescence Anisotropy to Support Groove Binding Event

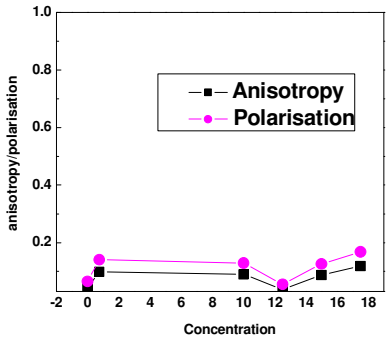

Figure S14: Fluoroscene anisotropy and polarization change of fluorophore in presence of various concentration of ct-DNA. [fluorophore] = 30 µM and [ct-DNA] =18,24, 30, 36 and 42 µM.

3.8. Macromodel calculation

The Macromodel calculation of the probe with a model DNA (**PDB Id: 1DNH**) was carried out by Maestro, version 9.0 with AMBER* force field in water.[3]

To support minor groove binding event, we have carried out MacoModel calculation. For the otimisation we have taken the DNA sequence [5'-d(*CP*GP*CP*GP*AP*AP*TP*TP*CP*GP*CP*G)-3', (**PDB Id: 1DNH**)] where Hoechst 33258 dye enter into the minor groove. Thus, Amber* optimized geometry of our probe phenoxazine with the model DNA sequence (**Figure S15**) showed and support our experimental observation of minor groove binding event.

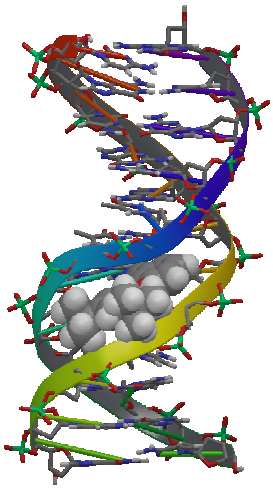

Figure S15: Amber* energy minimized geometry of the probe with DNA, showing the minor groove binding of the probe. The DNA sequence was 5'-d(*CP*GP*CP*GP*AP*AP*TP*TP*CP*GP*CP*G)-3', (**PDB Id: 1DNH**).

4. Theoretical Calculations

The ground state structures of the fluorophores were optimized using density functional theory (DFT) with B3LYP functional and 6-31G (d) basis set. The excited state related calculations were carried out with the Time dependent density functional theory (TD-DFT) with the optimized structure of the ground state (B3LYP/6-31G(d)). There are no imaginary frequencies in frequency analysis of all the calculated structures; therefore, each calculated structure is a local energy minimum.

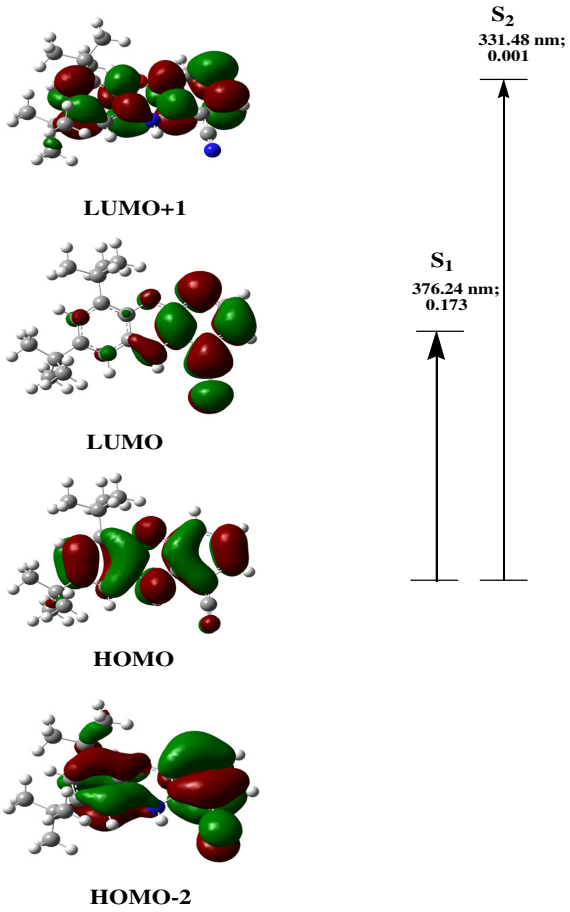

Figure S16: Excited-state energy levels of **1** based on TD-DFT calculations. The surface plots represent densities of the MOs with the largest contribution to the CI-eigenvectors.

Table 10: Summary of TD-DFT Calculation

Entry	Electronic transition	Energy (eV) (Wavelength)	*f*	Composition	CI
Phenoxazine	S_0 -> S_1	3.3765 eV 367.20 nm	0.1738	HOMO ->LUMO (86 -> 87)	0.65817
	S_0 -> S_2	3.7403 eV 331.48 nm	0.0017	HOMO ->LUMO+1 (86 -> 88)	0.67711

4.1. Cartesian Coordinates of the Optimised Geometry of phenoxazine

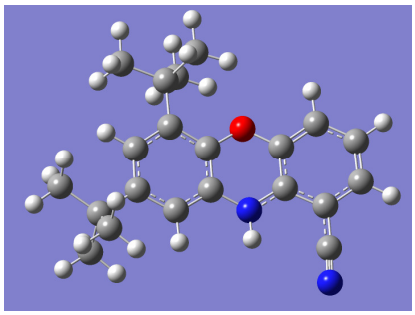

E(RB+HF-LYP) = -999.42166991 a.u.

Center Number	Atomic Number	Atomic Type	Coordinates (Angstroms) X	Y	Z
1	6	0	-1.220583	1.261609	-0.028312
2	6	0	0.133503	-0.767595	-0.157559
3	6	0	0.025571	0.631620	-0.123917
4	6	0	2.544130	-0.582708	-0.096093
5	6	0	-2.279856	-0.974566	-0.003206
6	6	0	-1.008184	-1.557238	-0.094367
7	1	0	-0.890053	-2.637530	-0.120330
8	6	0	-2.350667	0.420245	0.027015
9	1	0	-3.322142	0.885187	0.096982
10	6	0	3.834271	-1.138030	0.033166
11	6	0	2.412891	0.818244	-0.065475
12	6	0	3.521462	1.633625	0.083610
13	6	0	3.959405	-2.560078	0.016109
14	6	0	4.962661	-0.302046	0.174741
15	1	0	5.943364	-0.756306	0.265433
16	6	0	4.804345	1.072859	0.198823
17	6	0	-3.526043	-1.876923	0.062202
18	6	0	-4.832960	-1.067878	0.163090
19	1	0	-4.861397	-0.448269	1.066558
20	1	0	-4.977591	-0.415371	-0.705414
21	1	0	-5.686816	-1.753205	0.206170
22	6	0	-3.598832	-2.749186	-1.213823
23	1	0	-3.674838	-2.124906	-2.111321
24	1	0	-2.715216	-3.386575	-1.324870
25	1	0	-4.478122	-3.403967	-1.178835
26	6	0	-3.433171	-2.794950	1.304544
27	1	0	-4.313947	-3.445768	1.364265
28	1	0	-2.547372	-3.438245	1.273406
29	1	0	-3.383975	-2.203504	2.225885
30	7	0	1.407949	-1.344347	-0.261161
31	7	0	3.991903	-3.724883	-0.000551
32	8	0	1.178590	1.413647	-0.215577

33	1	0	1.489631	-2.350213	-0.191290
34	1	0	3.374426	2.708895	0.100708
35	1	0	5.666869	1.721942	0.307524
36	6	0	-1.361236	2.799866	0.006778
37	6	0	-0.615505	3.374129	1.236597
38	6	0	-0.793415	3.415339	-1.296141
39	6	0	-2.834774	3.242548	0.117818
40	1	0	-1.030990	2.967981	2.166263
41	1	0	0.451316	3.144764	1.210543
42	1	0	-0.729651	4.464788	1.265923
43	1	0	-1.339655	3.041494	-2.170089
44	1	0	-0.904425	4.506388	-1.272161
45	1	0	0.264665	3.183619	-1.430503
46	1	0	-2.878615	4.337039	0.141488
47	1	0	-3.432061	2.908826	-0.738089
48	1	0	-3.309171	2.875047	1.034750

References

1. C. Mukherjee, and S. Ghorai Chem. Commun., 2012 (in press) doi: 10.1039/C2CC35963D.
2. (a) Aposhian, H. V.; Kornberg, A. *J. Biol. Chem*. **1962**, *237*, 519. (b) Reichman, M. E.; Rice, S. A.; Thomas, C. A.; Doty, P. *J. Am. Chem. Soc*. **1954**, *76*, 3047.
3. Maestro, version 9.0, Schrödinger, LLC, New York, NY, 2009.

5. ^{1}H and ^{13}C NMR Spectra

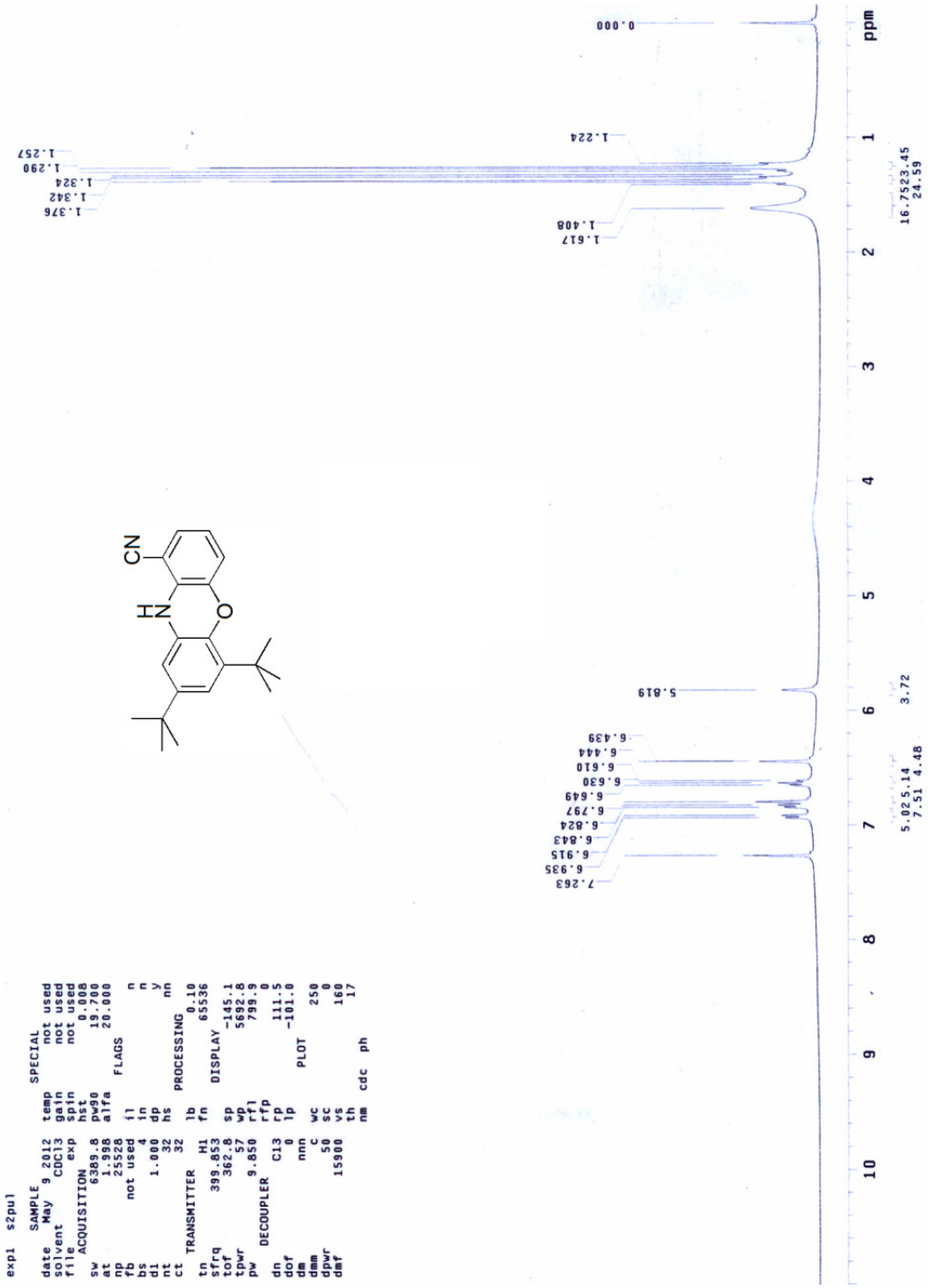

Figure S17: ^{1}H NMR of **1** measured in $CDCl_3$.

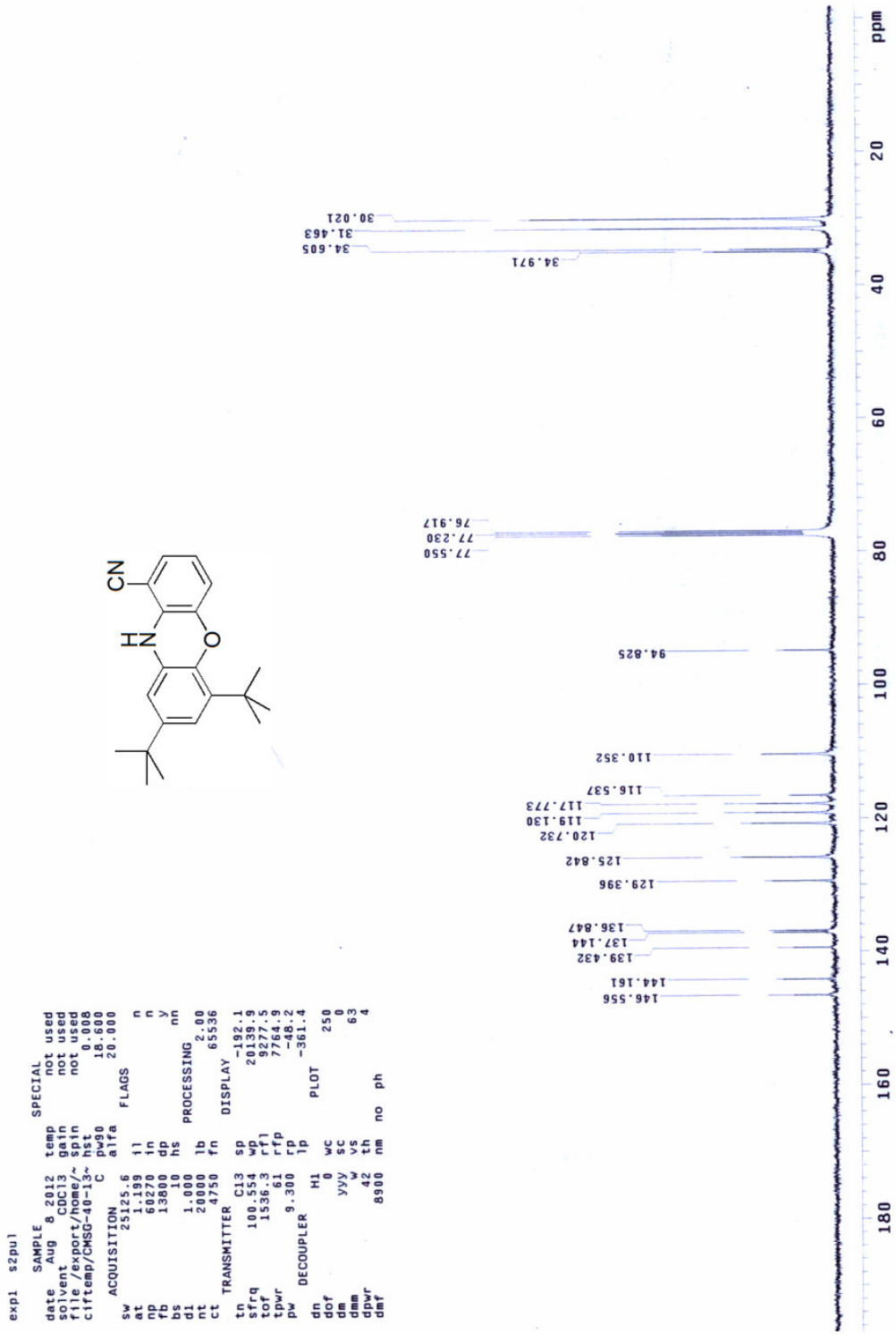

Figure S18: ^{13}C NMR of **1** measured in $CDCl_3$.